Indian Journal of Pure & Applied Physics
Vol. 60, November 2022, pp. 941-950
DOI: 10.56042/ijpap.v60i11.63670

Growth, Structural, Vibrational, Optical, Electrical and Thermal Properties of Transition Metal and Zinc Oxide added Glycine Semi-organic Crystal

P.Kavitha[a] & K. Sakthipandi[b*]

[a]Department of Physics, Mannar Thirumalai Naicker College, Pasumalai, Madurai 625 004, Tamil Nadu, India
[b]Department of Physics, SRM TRP Engineering College, Tiruchirappalli 621 105, Tamil Nadu, India

Received 2 June 2022; accepted 17 October 2022

The semi-organic crystals of the amino acid glycine were developed/grownup by the slow evaporation method from an aqueous solution in the manifestation/presence of zinc oxide and an additive Mn, Fe, Co, Ni, and Pb transition metals. Powder X-ray diffraction and elementary analyses of as-grown amino acid glycine crystals established/confirmed the existence of additive spices which sanctuary the basic crystalline structure of α-glycine. The energy dispersive x-ray analysis spectrum (EDAX) and scanning electron microscope (SEM) analysis were carried out to confirm the composition of elements present in the as-grown amino acid glycine crystals and to conclude the surface morphology. The existence/presence of functional groups and the nature of bonds present in as-grown amino acid glycine crystals were assigned by Fourier-transform infrared spectroscopy (FTIR) and micro-Raman spectrums. The optical transparency and cut-of wavelength have been predicted and the optical band gap of the ternary ZnO transition metal added crystals was calculated. The emission property of the crystals was analyzed by using a Photoluminescence study. The electrical properties of ZnO transition metallic additive added glycine semi-organic crystals were analysed using the impedance analyzer. The transition metals addition increases the conductivity of the glycine crystal. The dielectric analysis found that cultivated crystals were potential candidates for NLO applications. Thermal studies have shown that harvested semi-organic crystals have high thermal stability and high crystallization. The role of additives brings about significant changes in the physicochemical properties of semi-organic α-glycine crystals for promising applications of NLO.

Keywords: Transition metals; Semi-organic crystal; Slow evaporation; AC impedance; Conductivity.

1 Introduction

Semi-organic crystals provide experimental availability and can be easily adapted to each other's applications. Inherent instabilities hinder the use of pure organic crystals in industry and scientific studies because of oxidation in the air, dissolved/dissolution in acids, and easy damage. To overcome these limitations, the deposition of a protective shell was recommended as one of the possible methods for enhancing the physical and chemical stability of crystals[1,2]. Due to the plethora of optically active organic crystals, new semi-organic crystals have to be developed with high third-order nonlinearity and high mechanical and thermal stabilities for optical signal processing, wave mixing application, and optical sensors[3]. In recent years, semi-organic crystals, mainly organic matter added to transition metals, have fascinated considerable devotion due to their improved non-linear properties. A key feature/characteristic of using these semi-organic crystals/transition metallic additive added glycine semi-organic crystals for non-linear optics is their inimitable transfer of charge, either from metal/transition element to ligand or ligand to metal.

Because of the transfer of electron density between the metal atom and the conjugated ligand system, the metal-ligand bonding in semi-organic crystals is anticipated to exhibit high molecular hyper-polarizability[4,5]. The metal ions/ transition metal ions added crystals are currently receiving considerable attention as a result of the hurried expansion of laser diode industries[6]. Cultured crystals typically alter in terms of their physical characteristics under the effect of transitory metallic impurities in the crystalline matrix. In a growing field of materials chemistry, crystal growth of chemicals combined with transition metals has long been hindered by the particular synthetic difficulties associated with this form of crystal development[7]. In general, crystals added with various transition metal ions such as copper, iron, manganese, cobalt, etc., show a significant change in photorefractive properties and potential equipment

*Corresponding authors:
(Email: kavithamtnc@gmail.com; sakthipandi@gmail.com)

for holographic memories. Photo refraction and holographic quality depend upon the presence of defects due to growth conditions and deliberately with transitional metal ions[8,9]. In this study, the effect of ZnO with transition metal additives added with α-glycine is addressed. This work is specifically focused on studying the ability of the ternary compound of glycine, zinc oxide (GZnO), with the presence of various transition metals like Lead (Pb), Nickel (Ni), Cobalt (Co), Iron (Fe), and Manganese (Mn).

2 Synthesis and Characterization

In this study, using the solution growth technique, ZnO with transition metal added α-glycine semi-organic crystals have been grown/developed at room temperature from an aqueous solution. Sigma Aldrich chemicals such as glycine, zinc oxide and manganese chloride, ferric chloride, cobalt nitrate, nickel chloride and lead nitrate, and transition metal salts were purchased for this investigation. The required stoichiometric amount of glycine was measured and transferred to a beaker. A proportional stoichiometric quantity of ZnO was mixed with glycine and one of the transition metallic salts, known as $MnCl_2$. To obtain a homogeneous solution, the prepared mixed solutions were well dissolved in double distilled water and continuously stirred for 1 hour. Using Whatman filter paper, the stirred solution was filtered and enclosed with an aluminum sheet. Few gaps/ perforations have been carried out on the aluminum sheet to warrant controlled/well-ordered evaporation and keep the solution in a shielded/dust-free atmosphere. Likewise, other transitional metal salt solutions were prepared and stored for slow evaporation. Over the course of 35-45 days, transparent crystals were collected. The photocopy of the collected crystals can be found in Fig. 1. The addition of ZnO and manganese glycine is referred to as GZnO-Mn. Similarly, ZnO-iron, ZnO-cobalt, ZnO-nickel and ZnO-lead added glycine crystals were termed GZnO-Fe, GZnO-Co, GZnO-Ni and GZnO-Pb respectively. Cultivated crystals undergo structural, vibration, optical and electrical characterization.

The structural, vibrational, optical, electrical, and thermal properties of as-grown GZnO-Mn, GZnO-Fe, GZnO-Co, GZnO-Ni, and GZnO-Pb crystals were explored by using the following characterisation studies. A powder x-ray diffraction pattern of as-grown transition metal doped GZnO crystals was carried out using a D8 diffractometer with CuKα radiation (Bruker, USA; λ=1.54056 Aº). Fourier Transform Infrared

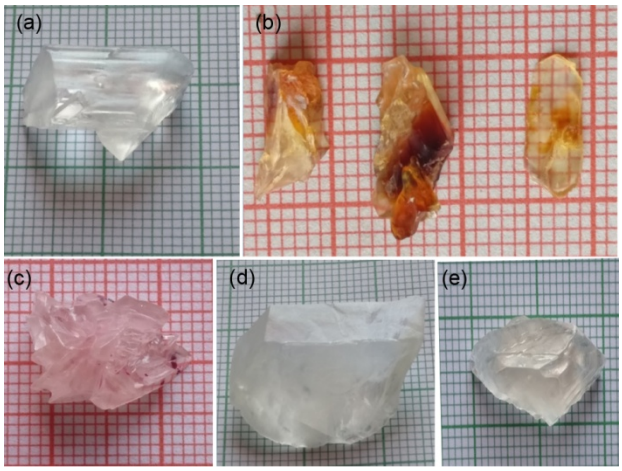

Fig. 1 — Photographs of the (a) GZnO-Mn, (b) GZnO-Fe (c) GZnO-Co, (d) GZnO-Ni and (e) GZnO-Pb cultivated crystals.

(FTIR) spectra of as-grown GZnO-Mn, GZnO-Fe, GZnO-Co, GZnO-Ni, and GZnO-Pb crystals were recorded in the range of 4000 – 400 cm^{-1} employing SHIMADZU FTIR spectrometer. The UV absorbance spectra of as-grown GZnO-Mn, GZnO-Fe, GZnO-Co, GZnO-Ni, and GZnO-Pb crystals were recorded using UV Systronics 2202 UV-Vis spectrophotometer in the range 200 - 800 nm. The photoluminescence properties of as-grown transition metal doped GZnO crystals were studied using ELICO SL-174 spectrometer. Using the impedance LCR HiTESTER analyzer (Hioki 3522-50 Japan), the electrical and dielectrical data of as-grown GZnO-Mn, GZnO-Fe, GZnO-Co, GZnO-Ni, and GZnO-Pb crystals were studied over a temperature range of 30 ºC to 70 ºC and a frequency range of 42 Hz to 10 MHz. Thermogravimetric analysis (TGA) and differential thermal analysis (DTA) spectra of as-grown transition metal doped GZnO crystals were taken using SDT Q600 thermal analyzer. The experiment was carried out in a nitrogen atmosphere at a heating rate of 10 ºC / min from room temperature to 800 ºC.

3 Results and Discussion

3.1 EDAX analysis

Figure 2 illustrates the EDAX spectrum of mixed ternary semi-organic crystals of GZnO-Mn, GZnO-Fe, GZnO-Co, GZnO-Ni and GZnO-Pb. The proportional elemental composition (in weight % ratio) of cultivated GZnO-Mn, GZnO-Fe, GZnO-Co, GZnO-Ni and GZnO-Pb crystals is presented in Table 1. The presence of all additives, the colour of the grown crystals and compositional weight percentage are explored in Figs. 1 & 2 & Table 1. SEM studies give the surface morphology of the cultivated

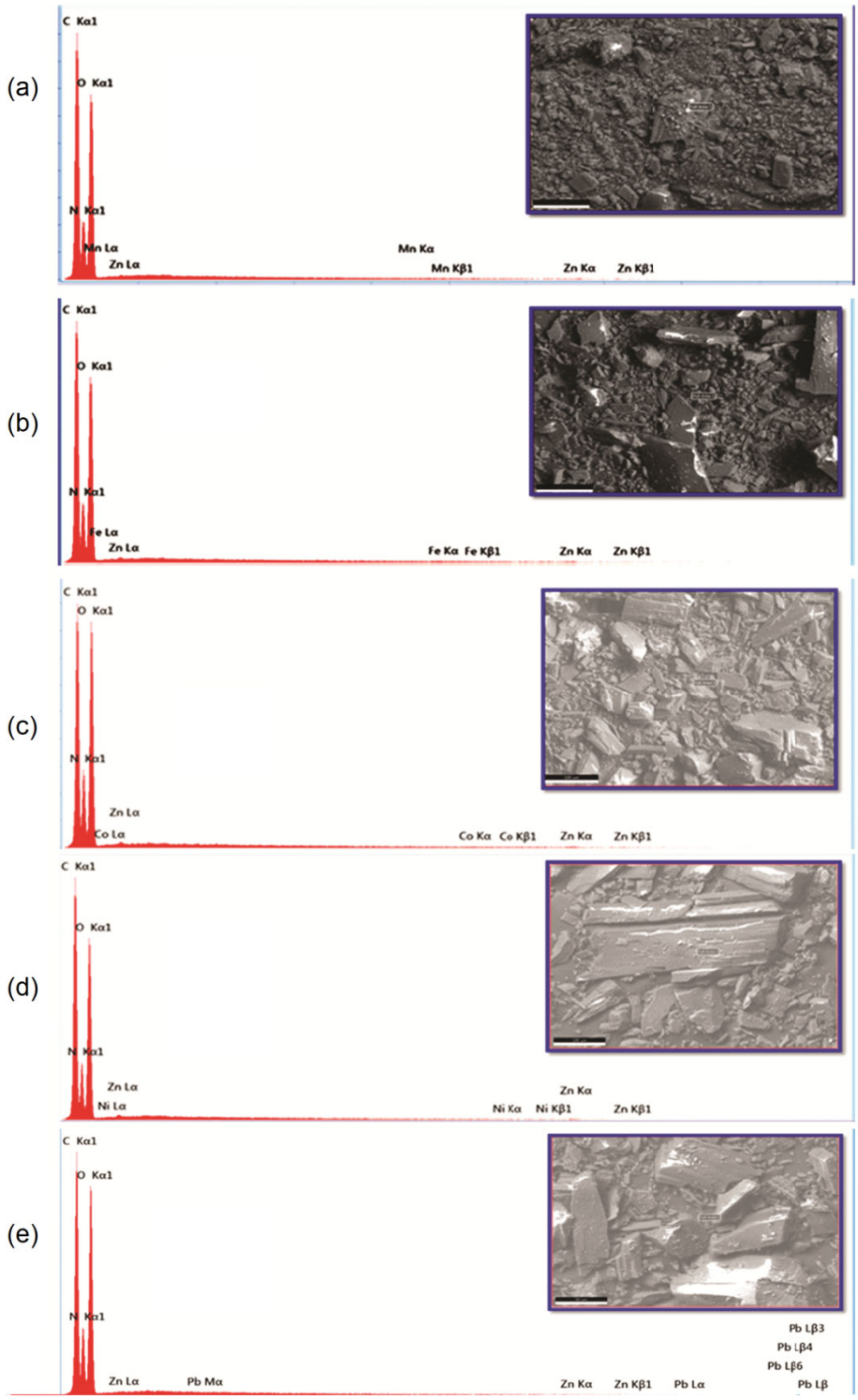

Fig. 2 — SEM and EDAX spectra of (a) GZnO-Mn, (b) GZnO-Fe, (c) GZnO-Co, (d) GZnO-Ni and (e) GZnO-Pb cultivated crystals.

GZnO-Mn, GZnO-Fe, bGZnO-Co, GZnO-Ni and GZnO-Pb crystals and the images are shown in the inset of Fig. 2. SEM micrographs of pure α-glycine crystals have shown a cloud-like exterior/ appearance because of the aggregation of the glycine crystals[10]. When ZnO is added with α-glycine, regular crystals of prismatic form with smooth surfaces have been obtained. This result is compatible with the

Table 1 — EDAX Spectra: Elemental composition of the GZnO-Mn, GZnO-Fe, GZnO-Co, GZnO-Ni and GZnO-Pb crystals.

Elements	Weight %				
	GZnO-Mn	GZnO-Fe	GZnO-Co	GZnO-Ni	GZnO-Pb
Colour of the crystal	Colorless &Transparent	Honey Brown	Pink	Colorless crystal	Colorless crystal
C	32.7	32.7	29.4	33.1	30.4
N	19.6	19.5	20.6	19.5	20.3
O	47.1	47.1	49.3	46.9	48.8
Zn	0.4	0.4	0.4	0.3	0.3
Transition element	Mn	Fe	Co	Ni	Pb
	0.2	0.3	0.2	0.2	0.2

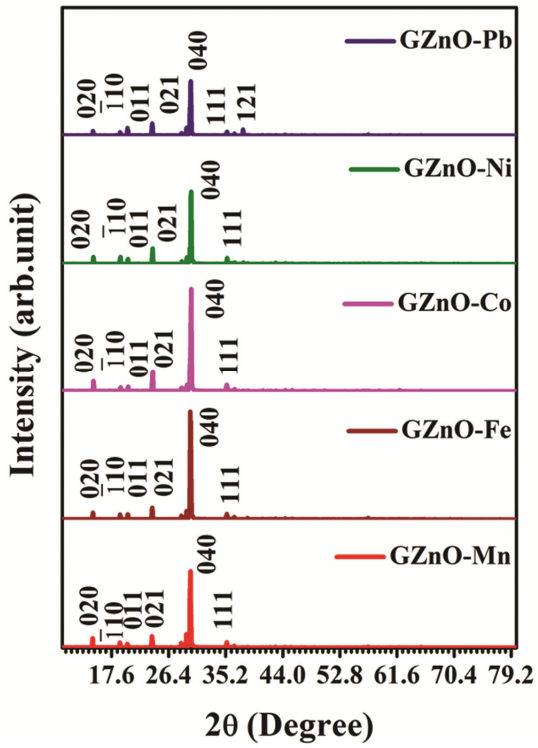

Fig. 3 — Indexed powder X-ray diffraction spectra of with Transition Metals added α-Glycine.

literature[11,12]. The ternary transition metal added semi-organic crystals had preserved prismatic morphology with a smooth surface of various sizes. The length and width of as-grown transition metal doped GZnO crystals have altered/changed in relation to the twofold ZnO-added glycine crystal.

3.2 Powder XRD analysis

The observed powder XRD patterns shown in Fig. 3, confirms the crystalline nature of the cultivated GZnO-Mn, GZnO-Fe, GZnO-Co, GZnO-Ni and GZnO-Pb crystals. XRD patterns are consistent with the reference JCPDS file #32-1702 of α-glycine. In general, it is expected that additives can reach interstitial lattice positions of the host crystal without

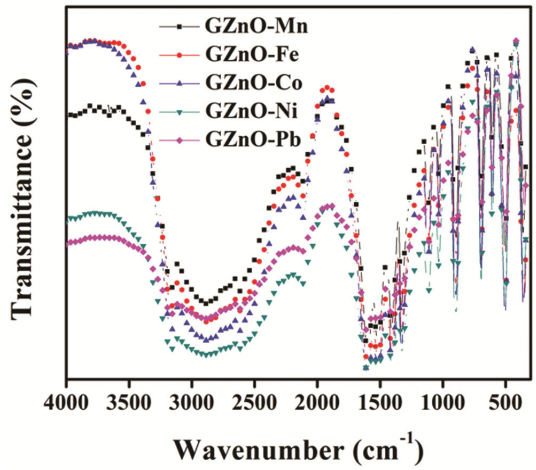

Fig. 4 — FT-IR spectra of ZnO with Transition Metals added α-Glycine.

affecting the lattice. It is evident from the XRD pattern shown in Fig. 3 that all the cultivated GZnO-Mn, GZnO-Fe, GZnO-Co, GZnO-Ni and GZnO-Pb crystals have the same growth direction in the (040) planes and the very high ZnO crystallinity with iron added GZnO-Fe glycine crystal. However, the GZnO-Co and GZnO-Ni glycine crystals have a different growth scheme in the (021) direction. As a result, the ternary addition of transition metals salts changed the glycine crystal's growth orientation. Although the growth directions and consequently the exterior shape of the crystals were altered in this study by the addition of ZnO and transition metal additions, the fundamental crystal structure of the -glycine single crystal was preserved[13].

3.3 FTIR and micro Raman analysis

Figs. 4 and 5 show the respectively FTIR and micro Raman spectrum of the cultivated GZnO-Mn, GZnO-Fe, GZnO-Co, GZnO-Ni and GZnO-Pb crystals in the 4000-400 cm^{-1} frequency region. It is hypothesized that the crystals' vibrational spectra shift as a result of the metal ion's interactions with organic

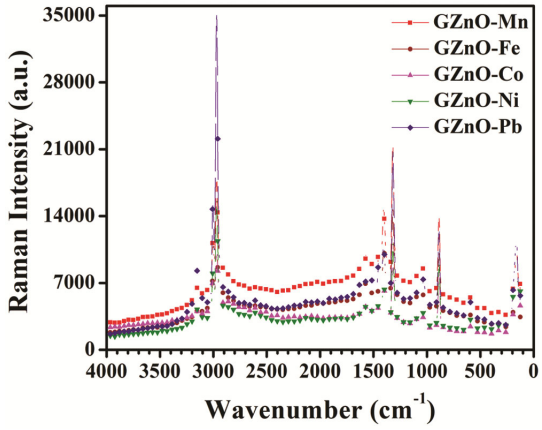

Fig. 5 — Micro Raman spectra of ZnO with Transition Metals added α-Glycine.

molecules. The alteration in vibration may be related to the alteration in individual frequency or molecule symmetry[14].CH_2 stretching vibrations create bands in the 3000–3100 cm^{-1} region[15-17]. The CH_2 stretch mode vibrations were obtained at 3140 cm^{-1} and 3130 cm^{-1} in the FTIR spectrum and micro-Ramon spectrum respectively. The stretching C=O mode was obtained at 1662 cm^{-1} in the micro Raman spectra[18]. The NH_2 rocking modes[19] occur at frequencies around 1100 cm^{-1}. The FTIR and micro Raman peak at 1033 and 1031 cm^{-1} was consigned to NH_2 rocking mode. The frequencies observed in the FTIR at 1577 cm^{-1} and in the micro Raman spectrum at 1588 cm^{-1} were allocated to C-C stretching vibrations[20,21]. Bands of the metal-O-metal group, which can absorb the entire region of 700-400 cm^{-1}, are present in several types of metal oxides[20,22]. Zn-O stretching vibration was seen as a strong FTIR peak at 694 cm^{-1} and 677 cm^{-1} in the micro Raman spectrum[14,23]. The peak at 502 and 482 cm^{-1} in the FTIR and micro Raman spectra were attributed to vibration υ (M-N)[24].

3.4 UV-Visible spectrum

Figure 6(a) presents the UV-Visible absorption spectra of the cultivated GZnO-Mn, GZnO-Fe, GZnO-Co, GZnO-Ni and GZnO-Pb crystals. The absorption peak was presented within the 200-210 nm (UV region) for all GZnO-Mn, GZnO-Fe, GZnO-Co, GZnO-Ni and GZnO-Pb crystals. However, the intensity of absorption for the GZnO-Fe crystal is greater than any other crystal. All the transition metal-doped GZnO crystals had good transparency across the visible region and near the infrared region. The band gap of the crystals was calculated/obtained from Tauc's plot of $(\alpha h\gamma)^{1/2}$ vs $(h\gamma)$ which shows the

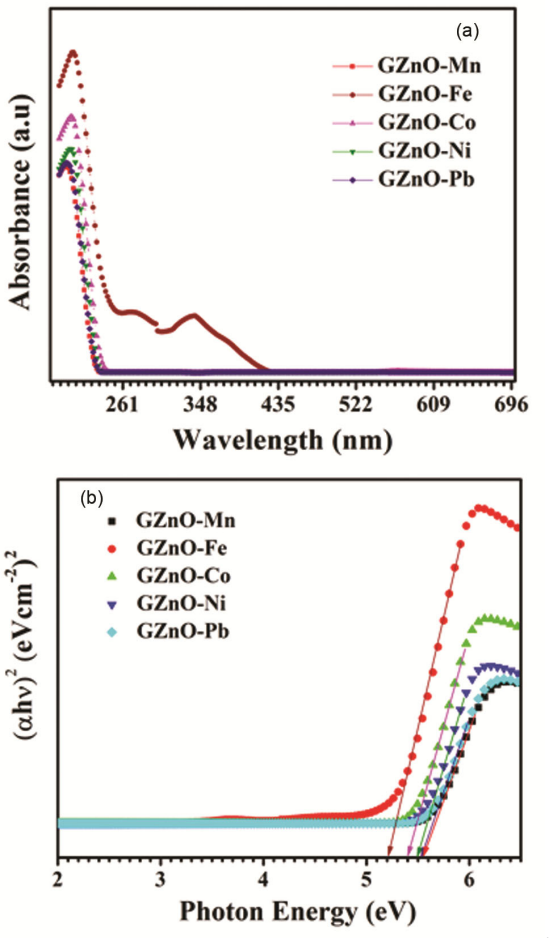

Fig. 6 — (a) UV-Visible spectrum and (b). Tauc's plot ZnO with Transition Metals added α-Glycine crystal.

crystals have a direct band gap. The energy band gap values of the crystals can be found by extrapolating linear lines in the plot.

From Fig. 6(b), the band gap values of the crystals GZnO-Mn, GZnO-Fe, GZnO-Co, GZnO-Ni and GZnO-Pb were found to be 5.55 eV, 5.2 eV, 5.4 eV, 5.5 eV and 5.55 eV respectively. The electrical conductivity is monitored by adjusting the energy bandwidth. The lowest band deviation of ZnO and Fe added glycine crystal shows the highest electrical conductivity among other cultured crystals. The emergence of divalent cations completes the additional holes in the valence band, which reduces the GZnO-Fe band interval[25]. The PL spectra of the cultivated GZnO-Mn, GZnO-Fe, GZnO-Co, GZnO-Ni and GZnO-Pb crystals are shown in Fig. 7. The emission intensity for GZnO-Mn and GZnO-Ni crystal in PL spectrum at 420 nm, when exited with 210 nm was higher that emission intensity of GZnO-Fe, GZnO-Co and GZnO-

Pb crystals. Cultured crystals are shown to emit a violet colour. The increased intensity could have been facilitated by energy charge transfer and cationic voids formed by transition metals[26].

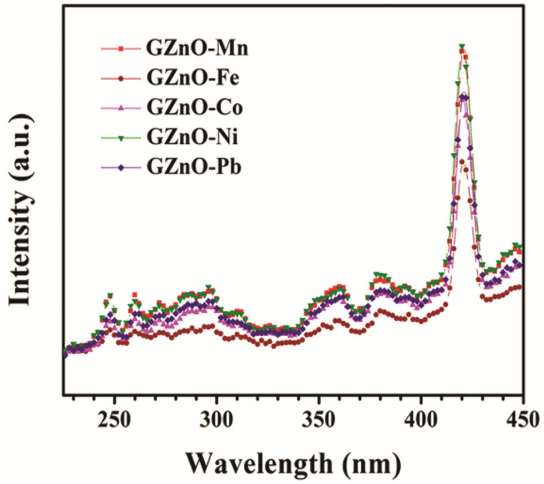

Fig. 7 — PL spectrum of ZnO with Transition Metals added α-Glycine crystal.

3.6 Electrical conductivity study

Electrical conductivity studies of crystals have improved understanding of the properties of materials for ion and electron transport. They provided information about these properties, such as AC conductivity and dependence on frequency and temperature. Fig. 8 depicts the impedance curve of the fictitious (imaginary) part Zsinθ against the fundamental part Zcosθ for the cultivated GZnO-Mn, GZnO-Fe, GZnO-Co, GZnO-Ni and GZnO-Pb crystals at various temperatures. The inherent characteristics expected the higher electrical conductivity of semi-organic transition metal and ZnO added glycine crystals than binary ZnO added glycine crystals (GZnO)[14]. In this analysis of the Cole-Cole plot, all cultivated GZnO-Mn, GZnO-Fe, GZnO-Co, GZnO-Ni and GZnO-Pb crystals were shown capacitive reactance and offered very low impedance in the high-frequency range. However, the semi-organic ZnO with cobalt-added glycine (GZnO-Co) crystal has demonstrated inductive reactance in the Cole-Cole plot, a novel criterion. Fig. 9 displays the AC conductance

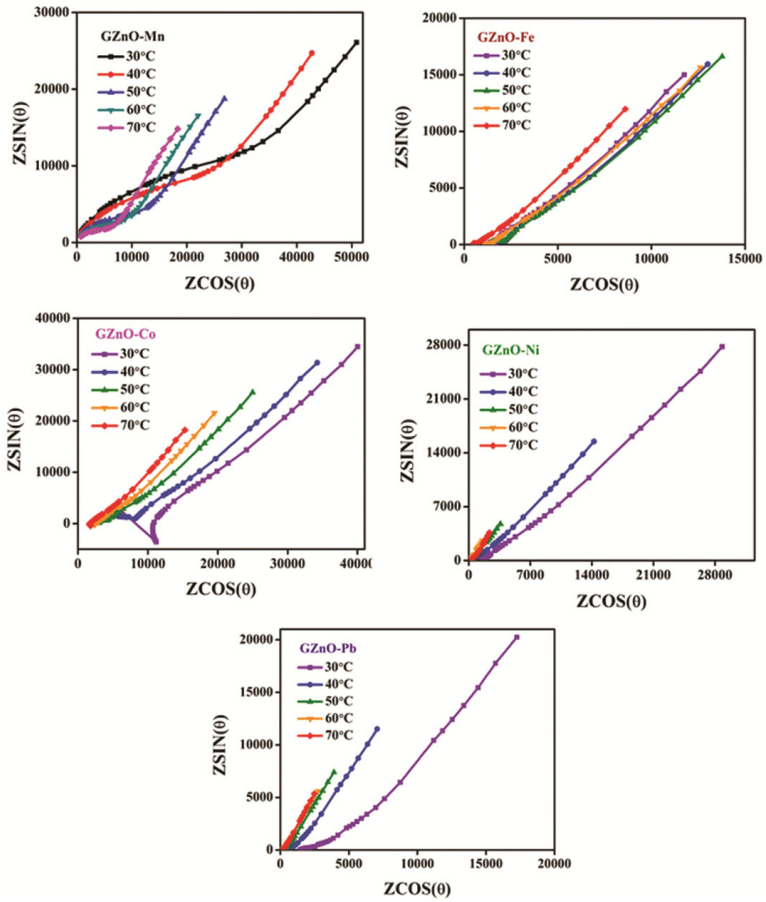

Fig. 8 — Impedance plot ZnO with Transition Metals added α-Glycine of crystals.

plots of cultivated GZnO-Mn, GZnO-Fe, GZnO-Co, GZnO-Ni and GZnO-Pb crystals that were measured in the 30 to 70 °C temperature range at 10 °C intervals. In the mid-frequency domain, the electrical conductivity of ternary mixed crystals was about ten times more than that of the binary glycine crystal, and it was more than 100 times greater in the high-frequency domain[14]. From Fig. 9, the conductivity increases at all temperatures due to the hopping of charges in the high-frequency region. Hence, the conductivity increases in transition metals added GZnO-Mn, GZnO-Fe, GZnO-Co, GZnO-Ni and GZnO-Pb crystals. The GZnO-Fe crystal has inflated electrical conductivity among all the grown crystals. The high conductivity mechanism is because of the hopping/skipping of Fe^{2+} and Fe^{3+} ions to the nearest sites[27]. Since the neighbouring oxygen atoms loosely bound the Fe^{2+} and Fe^{3+} ions, they can rapidly transfer/interchange to nearby vacancies because of the thermal activation process. Thus, the conductivity of the as-grown transition metal doped GZnO crystals increase as the divalent and trivalent cations movement increases[28]. The general electric study has indicated that ZnO and transition metal added glycine have high electrical conductivity than the pure glycine and ZnO added glycine crystal[14].

3.7 Dielectric studies

To study the lattice dynamics in the crystal, one must first understand the material's dielectric properties[25–29]. Due to different polarizations in solids, such as the electronic, space charge, orientational, and ionic polarizations, the dielectric constant and dielectric loss vary with temperature. Due to space charge polarisation, a high value of the dielectric constant is seen in the low-frequency zone. The space charge decreases as frequency rises, which results in decreasing values for the dielectric constant. According to Fig. 10, the dielectric constant first rises at lower frequencies and falls down exponentially when the frequency is added. The presence of space charge, orientation, and electronic and ionic polarisation often contribute to the dielectric constant's value at lower frequencies, whereas the regular loss of polarisation contributes to its low value at

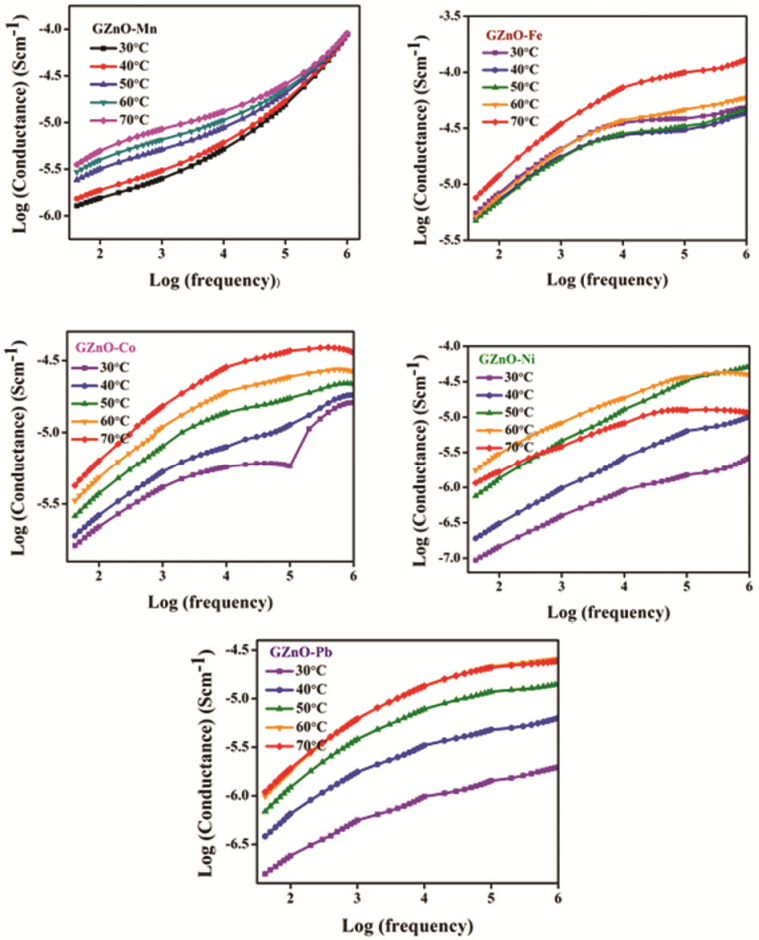

Fig. 9 — The conductance plot of ZnO with Transition Metals added α-Glycine of crystals.

higher frequencies[30]. The low-frequency domain's enhanced polarisation causes a rise in the dielectric constant. Contrarily, the low polarisation activity at higher frequencies has the effect of lowering the crystals' dielectric constant[31]. The dielectric constant of ternary mixed glycine crystals was found to be significantly lower than that of binary ZnO-added glycine crystals. When designing NLO, photonic, and electro-optic modulation devices, materials with lower dielectric constants consume less power[31]. In a crystalline material, the dissipation factor mostly depends on defect centres. Fig. 11 shows the dielectric loss profile of the cultivated GZnO-Mn, GZnO-Fe, GZnO-Co, GZnO-Ni and GZnO-Pb crystals. The ternary mixed crystals' lower dielectric loss suggested that the cultivated GZnO-Mn, GZnO-Fe, GZnO-Co, GZnO-Ni and GZnO-Pb crystals had more minor defect sites. The Miller rule[32] states that the low dielectric loss at high frequencies revealed the crystal's high optical quality and few electrically active flaws, which is a desirable characteristic for NLO applications. The produced semi-organic crystals were recommended for use in optoelectronic device applications due to their low dielectric constant and dielectric loss.

3.8 Thermal properties

Figure 12 shows the TG-DTA thermograms of GZnO-Mn, GZnO-Fe, GZnO-Co, GZnO-Ni and GZnO-Pb crystals. The TGA curves of all the crystals have shown no variation/change in weight up to 230 °C, which eliminates the probability of hydrate or solvent materialization of the crystals[33]. The crystals were stable up to 270 °C and weight loss was initialized above this temperature, which was evident from the exothermic peak at 270 ˚C in the DTA curves. The sharpness of the DTA peak indicates the degree of crystallinity of the samples. A considerable weight loss was observed in the region 240 °C – 280 °C. After this temperature, all the crystals have shown substantial weight loss in different steps. The lesser/smaller ionic radius of transition metals can spring more bonding interaction, and the internal bond energy increases, which offers more thermal stability to the ZnO and transition metal added glycine semi-organic crystals[34-36].

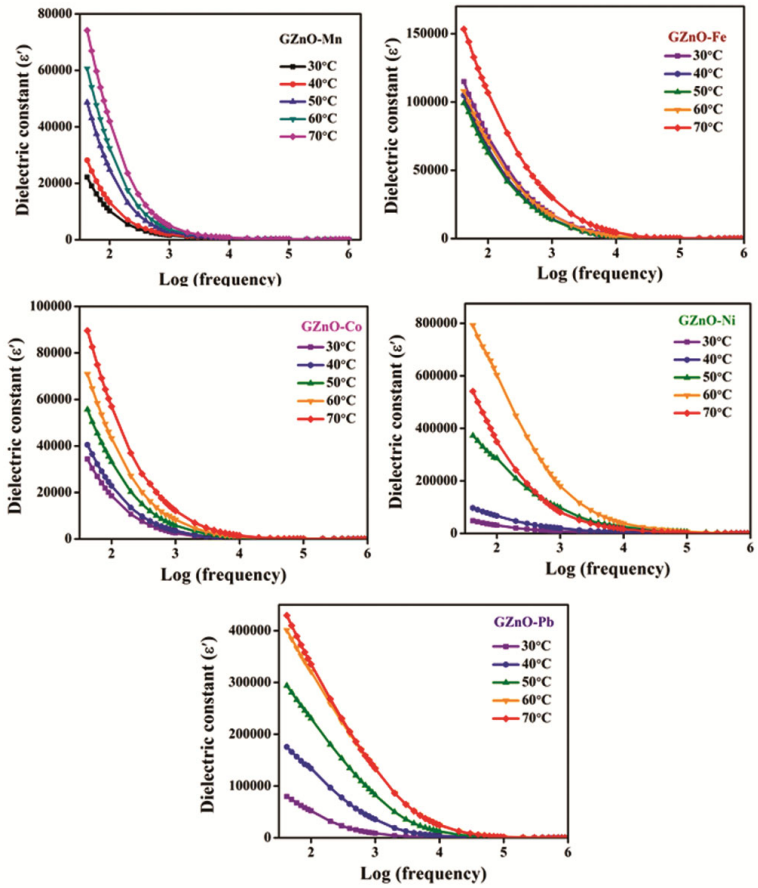

Fig. 10 — The profile of dielectric constant (ε') against frequency of ZnO with Transition Metals added α-Glycine of crystals.

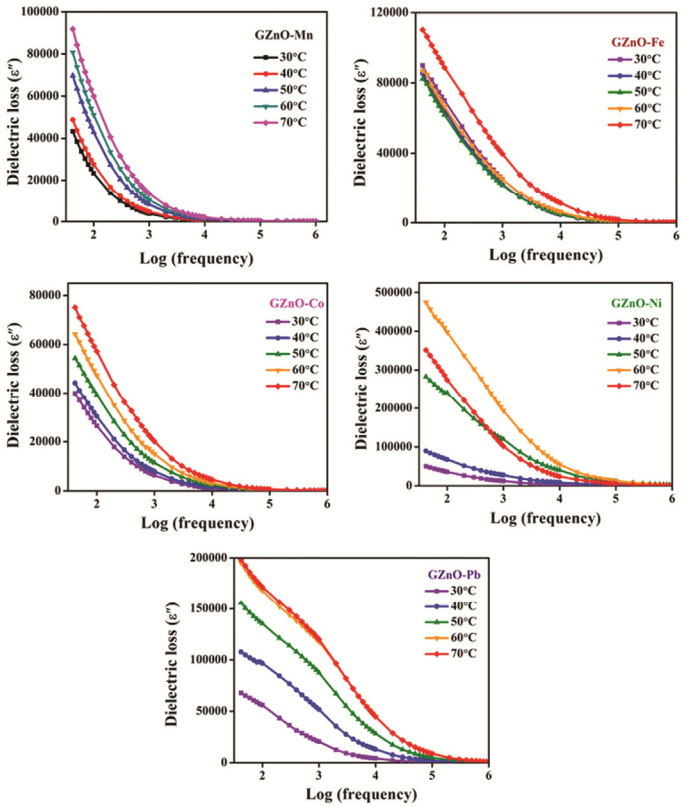

Fig. 11 — The profile of dielectric loss (ε") against frequency of ZnO with Transition Metals added α-Glycine of crystals.

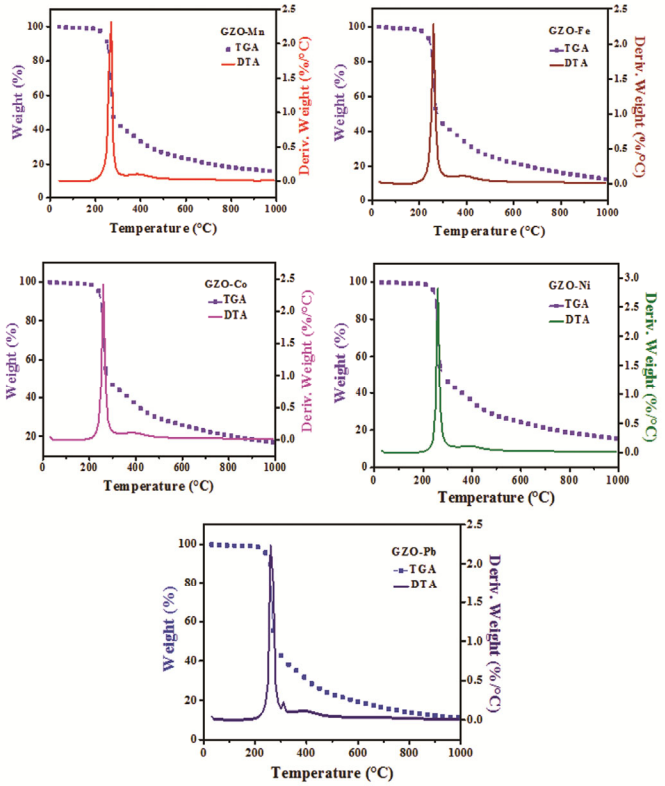

Fig. 12 — The TGA and DTA thermograms of ZnO with Transition Metals added α-Glycine of crystals.

4 Conclusions

The slow evaporation technique efficiently produces mixed semi-organic crystals of ZnO, α-glycine, and one of the transition metals (Mn, Fe, Co, Ni, and Pb) from an aqueous solution. According to structural analyses, the GZnO-Mn, GZnO-Fe, GZnO-Co, GZnO-Ni and GZnO-Pb crystals are having a single crystal of α--glycine with a monoclinic system and the space group P21/n. Without changing the α-glycine's fundamental structure, the additions of the transition metal reside in the crystal's interstitial space. The presence of various elements and the change in morphology of GZnO-Mn, GZnO-Fe, GZnO-Co, GZnO-Ni and GZnO-Pb crystals are confirmed by EDAX and SEM studies. The vibrational modes, presence of functional groups and nature of bonds/interactions between the molecules were confirmed by using FTIR and micro Raman analysis. The UV–Vis absorbance study exposed the cutoff wavelength of the crystals was found within 200-210 nm. All the GZnO-Mn, GZnO-Fe, GZnO-Co, GZnO-Ni and GZnO-Pb crystals are transparent in the entire visible region. Hence, ZnO with transition metals added to glycine crystals is very much useful for optical applications. PL emission of crystals was tested and cultivated crystals showed violet emission. The results of the dielectric measurement showed that the dielectric constant and loss value was low at high frequencies and decreased with temperature. The thermal steadiness of the as-grown transition metal doped GZnO crystals indicated that the crystal has good thermal stability up to 270 °C. The low dielectric constant and low dielectric loss values have been obtained for GZnO-Mn, GZnO-Fe, GZnO-Co, GZnO-Ni and GZnO-Pb. Thus the ZnO with transition metals added to glycine crystals crystal can be utilized for optoelectronic applications.

References

1 Galaburda M, Bogatyrov V, Oranska O, Gunko V, Skubiszewska-Zie J & Urubkov I, *J Therm Anal Calorim*, 122 (2015) 553.
2 Ibrahim M J & Al-Saadi T M, *AIP Conf Proc*, 2123 (2019) 020015.
3 Sagunthala P & Yasotha P, *SN Appl Sci J*, 1 (2019) 1109.
4 Sun H Q, Yuan D R, Wang X Q, Lu Y Q, Sun Z H, Wei X C, Duan X L, Luan C N, Lu M K & Xu D, *J Cryst Growth,* 256 (2003) 183.
5 Ushasree P M, Muralidharan R, Jayavel R & Ramasamy P, *J Cryst Growth,* 197 (1999) 216.
6 Kaur P, Kriti, Kaur S, Arora D, Rahul, Kandasami A & Singh D P, *Mater Res Express*, 6 (2019) 115920.
7 Cortese J, Abeysinghe D, Smith M D & Loye H C, *J Solid State Chem*, 240 (2016) 76.
8 Kar S, Verma S & Bartwal K S, *Cryst Growth Des*, 8 (2008) 12.
9 Sinha N, Ray G, Godara S, Yadav H, Bhandari S & Kumar B, *Physica B*, 470 (2015) 15.
10 Arockia A S & Leo R A, *J Mater Sci Mater Electron*, 28 (2017) 10893.
11 Tari T, Ambrus R, Szakonyi G, Madarasz D, Frohberg P, Csoka I, Szabo-Revesz P, Ulrich J & Aigner Z, *Chem Eng Technol*, 40 (2017) 1323.
12 Nii S & Takayanagi S, *Ultrason Sonochem*, 21 (2014) 1182.
13 Benila B S, Bright K C, Mary Delphine S & Shab R, *Opt Quant Electron,* 50 (2018) 202.
14 Kavitha P, Venkatesh B N & Ramaswamy S, *AIP Conf Proc,* 2162 (2019) 020046.
15 *Beena T, Sudha L, Nataraj A, Balachandran V, Kannan D & Ponnuswamy M N, Chem Cent J,* 6 (2017) 11.
16 Nath M J, Roy S D D & Joe I H, *J Phys Chem Solids*, 122 (2018) 143.
17 George J, Sajan D, Alex J, Aravind A, Vinitha G & Chitra R, *Opt Laser Technol*, 105 (2018) 207.
18 Vediyappan S, Raja A, Jauhar R M, Kasthuri R, Vijayan V, Pandian M S, Ramasamy P & Vinitha G, *J Mater Sci Mater Electron*, 32 (2021) 15026.
19 Mohamed A R, Premkumar S, Mathavan T & Milton F B A, *J Mol Struct*, 1134 (2017) 143.
20 Chitrambalam S, Manimaran D, Hubert J I, Rastogi V K, Hassan I Ul, *Opt Mater,* 75 (2018) 285.
21 Sangeetha P, Jayaprakash P, Nageshwari M, Kumari R T C, Sudha S, Prakash M, Vinitha G & Lydia C M, *Phys B*, 525 (2017) 164.
22 Ryohei H, Nagato E, Takayuki A, Yuta M, Takuya S, Kazuki Y, Satoru T & Takahiro G, *J Solgel Sci Technol*, 87 (2018) 743.
23 Jabeen M, Ahmad S, Shahid K, Sadiq A & Rashid U, *Front Chem*, 6 (2018) 1.
24 Zarrin N & Husain S, *Appl Phys A*, 124 (2018) 730.
25 Ramteke S P, Mohd A, Baig M I & Muley G G, *Optik*, 154 (2018) 275.
26 Marimuthu A & Perumal R N, *J Alloys Comp*, 869 (2021) 159284.
27 Gavalda J, Carvajal J J, Mateos X, Aguilo M & Diaz F, *Appl Phys Lett*, 95 (2009) 182902.
28 Rajagopalan N R & Krishnamoorthy P, *Optik,* 129 (2017) 118.
29 Manivannan M, Martin B D S A & Jose M, *J Cryst Growth*, 455 (2016) 161.
30 Shaikh R N, Mohd A, Shirsat M D & Hussaini S S, *J Optoelectron Adv*, 16 (2014) 1147.
31 Mohd A, Shirsat M D, Hussaini S S, Joshi B & Muley G G, *J Mater Sci Technol*, 32 (2016) 62.
32 Miller R C, *Appl Phys Lett*, 5 (1964) 17.
33 Uma J & Rajendran V, *Optik,* 125 (2014) 816.
34 Benila B S, Bright K C, Mary D S & Shab R, *Opt Quant Electron,* 50 (2018) 202.
35 Sangeetha S & Rajendran V, *J Alloys Compd*, 789 (2019) 1008.
36 Kumar A R, Ezhil V R, Vijayan N & Rajan B D, *Physica B,* 406 (2011) 2594.